Molecular Chemisorption on TiO_2(110): A Local Point of View

M. Casarin and C. Maccato

Dipartimento di Chimica Inorganica, Metallorganica ed Analitica, via Loredan 4, I-35131 Padova, Italy

A. Vittadini*,†

CSSRCC CNR, via Marzolo 1, I-35131 Padova, Italy

Received: March 4, 1998; In Final Form: July 29, 1998

The molecular adsorption of some probe molecules (CO, H_2O, and H_2S) on a 5-fold-coordinated Ti Lewis acid site of the TiO_2 rutile (110) surface is studied within the density functional theory. The substrate is modeled with a small Ti_7O_9 cluster terminated with pseudo-hydrogens. This is found to describe the electronic and structural properties of the clean surface in good agreement with both experimental and periodic slab calculations. Adsorption energies (6.7, 19.3, and 7.0 kcal/mol for CO, H_2O, and H_2S, respectively) and adsorbate stretching frequencies compare favorably with available experimental data. The agreement is particularly good for the C−O stretching frequency shift (+56 cm^{-1}), as was found in previous investigations carried out with the same theoretical approach on other oxides. In contrast, the HOH scissoring mode is poorly reproduced, suggesting that molecularly adsorbed H_2O is actually involved in weak bonds with other adsorbed species. This agrees with predictions of very recent slab calculations by Lindan et al. (*Phys. Rev. Lett.* **1998**, *80*, 762). Differences with respect to calculations carried out by embedding the cluster in point-charge arrays are discussed.

1. Introduction

An understanding of the interactions between TiO_2 surfaces and molecules is important because they are involved in a number of technological processes, such as photocatalytic water splitting.[1] Recent advances in photocatalysis on TiO_2 have been reviewed by Linsebigler et al.[2] The availability of new algorithms and fast computers has recently allowed the feasibility of theoretical calculations of TiO_2 surface structures and properties which are in excellent agreement with experimental data.[3,4] However, these calculations, based on periodically repeated slabs, are computationally demanding, and they are not very efficient, e.g., for calculating adsorbate vibrations. Realistic cluster models are still useful in such cases, even though they have not been found to be always adequate. For instance, an overly large stretching-frequency shift was predicted for molecularly adsorbed CO.[5] In this paper, we intend to show that small clusters terminated with pseudo-hydrogens are able to model adequately the molecular adsorption of some simple molecules (CO, H_2O, and H_2S) on the TiO_2(110) surface, as we already have shown for the surfaces of other oxides and ionic materials.[6−9]

2. Computational Method

Model. The surface was modeled with a Ti_7O_9 cluster, centered on a 5-fold-coordinated Ti surface ion, which is assumed to be the adsorption site. A sketch of the cluster is reported in Figure 1, where oxygen atoms are labeled according to ref 10 and the *x*, *y*, and *z* axes correspond respectively to the [001], [$\bar{1}$10], and [110] crystallographic directions. The experimental lattice constants (a = 4.593 Å, c = 2.959 Å) were used.[1] In building cluster models, one has to solve the problem of getting rid of spurious surface states originated by dangling bonds (DBs) in the gap. In principle, one could simply take very large clusters, but this is only possible in semiempirical approaches.[12] Most often, one takes small clusters and imposes upon them some boundary conditions. Point-charge (PC) arrays are widely used for this purpose, even though choosing the "best" values for PCs is almost a matter of taste: typically adopted values range from the Mulliken charges to the substantially higher formal oxidation numbers. However, it is well-known that the Mulliken charge density analysis, which is one of the most popular procedures for these purposes, is rather arbitrary. More realistic charge partitioning schemes, like that of Hirshfeld,[13] usually provide lower ionicities. The use of overly high PC values may cause unwanted consequences, such as an excessive polarization of DB electrons, and the generation of overly strong Madelung fields at surface sites. On the other hand, low PC values can be unable to embed properly the DB states.[14] An alternative way of treating the DBs is the adoption of pseudo-hydrogens carrying a fractional charge. We have

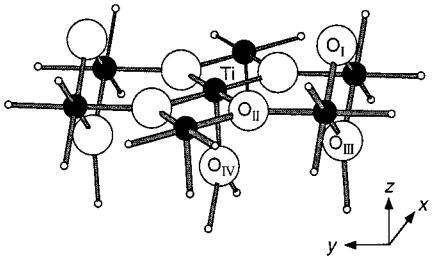

Figure 1. Schematic structure of the model cluster. Dark circles represent Ti atoms, white circles represent O atoms, and small white circles represent saturators.

* To whom correspondence should be addressed.
† E-mail: vittadini@chim02.unipd.it.

10.1021/jp981377i CCC: $15.00
Published on Web 12/02/1998

successfully applied this approach to model surfaces of ZnO,[6] Cu_2O,[7] CuCl,[8] and Ag_2O.[9]

For this study, we proceeded as follows. We first point out that in the rutile TiO_2 structure Ti^{4+} ions are 6-fold-coordinated, but those of O^{2-} are 3-fold-coordinated. This means that each Ti shares its four valence electrons with six oxygens, thus contributing with $^2/_3$ of an electron to each metal−oxygen bond. On the other hand, because of its planar configuration, each O keeps two electrons as a lone pair, and so, it is able to give $^4/_3$ of an electron to each Ti−O bond. Therefore, if we want to saturate correctly the cluster, we have to provide $^4/_3$ of an electron to each Ti DB and $^2/_3$ of one to each O DB. This result can be achieved by using pseudo-hydrogen saturators with fractional nuclear charges (H′ with $Z = {}^4/_3$, and H″ with $Z = {}^2/_3$). These saturators have been found to be very well-suited for terminating TiO_2 clusters, allowing a fast convergence with cluster size.[15] The pseudo-hydrogens are placed along the bond directions of the extended lattice; distances from cluster ions are determined by optimizing the geometries of TiH'_6 and OH''_3 "pseudomolecules". We wish to point out that pseudo-hydrogen saturators are treated exactly like all of the other cluster atoms; i.e., they contribute not only to the cluster potential but also to the cluster charge. Therefore, they should not be confused with the pseudoatoms adopted in ref 16.

We then had to determine the correct number of electrons to fill the cluster levels. On the (110) surface, an equal number of 2-fold-coordinated O and 5-fold-coordinated Ti is present. The charge of Ti DBs is transferred to the O DBs, which are filled with two electrons. However, in our cluster, the number of coordinatively unsaturated cations is higher than that of the anions, thus, we have to force the removal of the charge corresponding to the extra Ti DB (i.e., $^2/_3$ of an electron) from the cluster states. We emphasize that providing a correct population for the DBs is essential to set up physically sound models of surfaces; otherwise, unpredictable errors can occur in computing adsorption energies.[17] This could be done simply by taking a charged cluster ($+{}^2/_3$ in this case), as in refs 6−9. For this work, we have chosen a different approach. Actually, replacing two of the H′ saturators by two H atoms implies the removal of exactly $^2/_3$ of an electron from the cluster levels, without affecting the net charge of the system. This is preferable from some points of view (e.g., no arbitrary shifts are needed to compare one-electron levels). The saturators replaced were those at the bottom of the Ti atoms lying along the *x* axis (see Figure 1). The validity of our choice was checked by trying the alternative, isolobal OH fragments: test calculations showed that chemisorption energies and vibrations of adsorbates at the Lewis acid site were not affected by the substituent change.

We also carried out calculations on a Ti_7O_9 cluster embedded in an array of 590 PCs. The same +10 net charge, deduced from the formal ion charges, was assigned to the cluster, when using both a (+4/−2)[18] PC array and "Mulliken-like" (+2/−1) PC array. This was absolutely needed to avoid the introduction of spurious, additional levels in the gap. The overall electroneutrality of the system was ensured in the latter case by slightly adjusting the charge of the negative PCs.

Computational Details. Our calculations were performed within the density functional theory (DFT) approach, by using the ADF 2.0.1 and ADF 2.3.0 packages.[19,20] Geometry optimizations and frequency calculations were run using the local density approximation (LDA), and total energies were obtained by means of generalized gradient (GGA) corrections self-consistently included through the Becke−Perdew (BP) formulas.[21] BP GGAs are known to improve significantly the agreement of metal−ligand binding energies[22] and of adsorption energies[23] with experimental data and have been also successfully employed in recent slab calculations[10] on TiO_2(110).

TABLE 1: Atomic Displacements (Å) from the Bulk Compared with Experiment and Various Slab Calculations

atom	this work	exptl[a]	LDA-PW[b]	FLAPW[c]	HF[d]	GGA-PW[e]
Ti(z)	−0.20	−0.16	−0.17	−0.18	−0.15	−0.11
O_I(z)	−0.13	−0.27	−0.07	−0.16	−0.14	−0.02
O_{II}(y)	+0.04	+0.16		+0.07	+0.08	+0.05
O_{II}(z)	+0.09	+0.05	+0.13	−0.12	+0.07	+0.18

[a] From ref 3. [b] From ref 4. [c] From ref 27. [d] From ref 28. [e] From ref 29.

A triple-ζ Slater-type basis set was used for all of the adsorbate atoms and for titanium atoms, and for the oxygen lattice atoms, we used a double-ζ basis. Pseudo-hydrogens were described by a single-ζ basis. The inner cores of titanium and sulfur (1s2s2p), as well as oxygen and carbon (1s), were treated by the frozen-core approximation. We verified that basis sets of this quality give results identical to our previous LDA calculations performed on Cu_2O with the DMol package.[7]

The adsorption energy (ΔH_{ads}) was analyzed in terms of the adsorbate and surface fragment orbitals, applying Ziegler's generalized transition-state method:[24]

$$\Delta H_{ads} = \Delta E_{elstat} + \Delta E_{Pauli} + \Delta E_{int} + \Delta E_{prep}$$

where ΔE_{elstat} is the pure electrostatic interaction, ΔE_{Pauli} is the Pauli repulsion, ΔE_{int} is the orbital interaction, and finally, ΔE_{prep} is related to the geometry deformation undergone by the free fragments in the interacting system. ΔE_{int} is broken down in symmetry contributions (a_1, a_2, b_1, and b_2 in the C_{2v} symmetry adopted for calculations herein reported).

Final adsorption energies were corrected taking into account the basis set superposition error (BSSE). This was estimated making use of reference energies calculated with "ghost" adsorbate and surface fragments.[25]

Density of states (DOS), partial density of states (PDOS), and crystal orbital overlap population (COOP)[26] curves have been computed by applying a 0.25-eV Lorentzian broadening to the eigenvalues of the clusters. The PDOS and COOP curves are obtained by weighting the one-electron levels by their basis orbital percentage and by the overlap population between (sets of) orbitals, respectively. These curves provide information about the localization and the bonding/antibonding character of the molecular orbitals (MOs).

3. The Clean Surface

We first checked the ability of the cluster to mimic correctly the properties of the clean surface. The first test was an analysis of the atom relaxations. For this purpose, we allowed all of the surface ions not directly bonded to pseudo-hydrogen saturators to relax. The obtained displacements are collected in Table 1, where the experimental[3] and the theoretical values (obtained from several slab calculations[4,27−29]) are reported for comparison. The agreement between theoretical and experimental values is surprisingly good, given the limited dimensions of our model. In particular, we emphasize that *all* of the displacements are in the right direction. Furthermore, differences between our results and those obtained from slab models appear to be of the same order as differences between different slab calculations. This may indicate that the accuracy of the local description of the potential is more important than the inclusion of long-range effects.

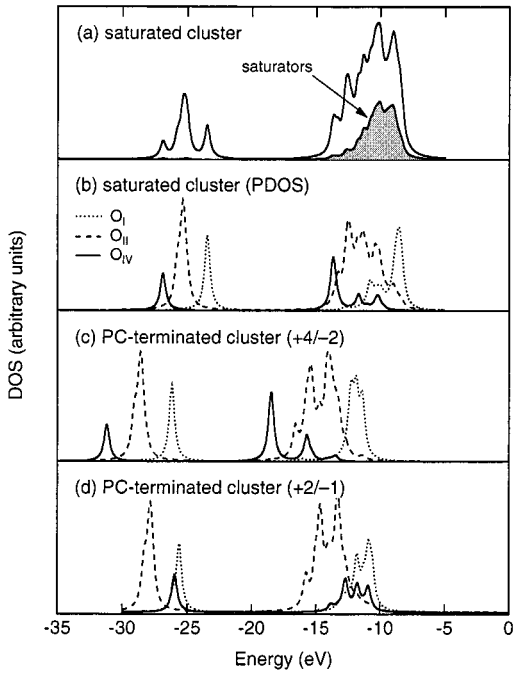

Figure 2. (a) DOS of the pseudo-hydrogen-saturated model cluster. The shaded area shows the contribution from the saturators. (b) PDOS from O atoms of the same cluster. (c) PDOS of the cluster terminated with the (+4/−2) PC array. (d) PDOS of the cluster terminated with the (+2/−1) PC array. Only occupied states are displayed in this panel.

Because we allowed only the vertical position of the central Ti ion to vary in the molecular adsorption calculations, we repeated our calculations on the bare cluster and optimized only this degree of freedom to obtain a consistent reference state. The relaxation was found to increase slightly under these conditions ($\Delta z = -0.22$ vs -0.20 Å). The GGA DOS curve of the optimized system is reported in Figure 2a. The curve is composed of two main bands, centered at ∼−25 and ∼−10 eV, related to the O 2s and O 2p atomic orbitals (AOs), respectively. It can be appreciated that the local DOS of the saturators gives a large contribution to the total DOS, it does not change substantially the shape of the curve. This is an early indication that the pseudoatoms are well-suited for their purpose. In Figure 2b, we report the PDOS pertinent to the O_I, O_{II}, and O_{IV} anions.

Comparisons among the saturated PDOS curves and those obtained from calculations where the Ti_7O_9 cluster is terminated with PC arrays provide interesting data. The curves obtained from the PC-terminated clusters, reported in Figure 2c,d, differ appreciably from those of Figure 2b. In particular, the O_I 2p PDOS forms a single peak in Figure 2c whereas in the pseudo-hydrogen saturated cluster it is clearly split into two components. Furthermore, the peaks related to the O_{IV} 2s and 2p states are heavily influenced by the charges assumed for the PCs: In the (+4/−2) case, they are overstabilized, and in the (+2/−1) case, they are unphysically found to be degenerate with the O_{II} peaks. In both cases, there is a disagreement with DOS of ref 10, suggesting that the pseudo-hydrogen termination allows a more realistic description of the surface electronic properties. Also, the comparison with photoemission spectra is more favorable for the pseudo-hydrogen saturation.

As far as the charges of the cluster ions are concerned (see Table 2), the Mulliken analysis provides values similar to those reported in the literature,[5,28] but the Hirshfeld estimates are sensibly lower (∼−0.3 for oxygens and ∼+0.6 for Ti). Thus, a realistic electrostatic embedding field may require charge values much lower than the formal valence charge values.

TABLE 2: Gross Mulliken and Hirshfeld Charges of the Chemically Complete Atoms Obtained with the Pseudo-hydrogen Saturation (PS) and with the (+4/−2) Point-Charge Embedding (PC)

	Mulliken		Hirshfeld	
atom	PS	PC	PS	PC
Ti	+2.15	+2.00	+0.67	+0.68
O_I	−0.82	−0.82	−0.31	−0.15
O_{II}	−1.03	−1.05	−0.30	−0.19

TABLE 3: Structural and Vibrational Properties of Free and Adsorbed (Saturated Cluster) CO as Obtained from LDA Calculations

	theor	exptl
free CO		
r_{CO} (Å)	1.132	1.127[a]
υ_{CO} (cm^{-1})	2156	2143[a]
adsorbed CO		
r_{CO} (Å)	1.126	
r_{Ti-CO} (Å)	2.344	
Δz_{Ti} (Å)	−0.191	
υ_{CO} (cm^{-1})	2212	2186/2206[b]
υ_{Ti-CO} (cm^{-1})	187	
$\Delta\upsilon_{CO}$ (cm^{-1})	+56	+40/+60

[a] From ref 31. [b] From ref 32.

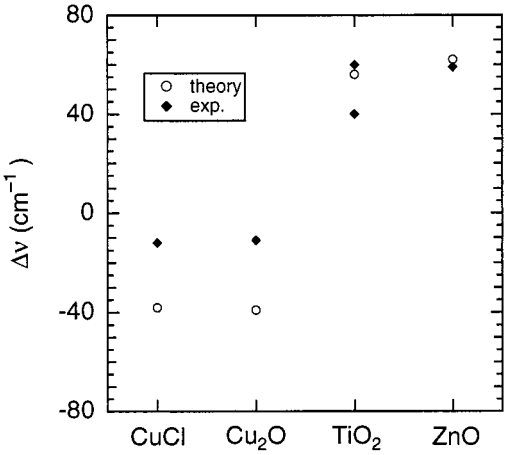

Figure 3. Plot of the experimental[7,32,33] (diamonds) and theoretical[6−8] (open circles) C−O stretching-frequency shift ($\Delta\nu$) for CuCl, Cu_2O, TiO_2, and ZnO.

4. Molecular Adsorption of CO

In these calculations, we placed on top of the central Ti ion[30] a CO molecule oriented with the C down. Only the vertical coordinate of the ion and those of the atoms belonging to the adsorbate were allowed to relax. The structural and vibrational properties of CO in the free and the adsorbed states are reported in Table 3. Both the adsorbate and the substrate structures are found to be only slightly perturbed with respect to the free fragments. The agreement with available experimental data[31,32] is very good. In particular, the experimental 40−60-cm^{-1} blueshift of the C−O stretching frequency ($\Delta\nu$) measured on powdered rutile samples[32] is strikingly reproduced. We believe that this is not fortuitous, as can be inferred from Figure 3, where the experimental trends of $\Delta\nu$ for some oxide and ionic materials[8,33] are plotted together with our estimates from LDA calculations carried out in ways similar to the present ones.[6−8]

TABLE 4: Theoretical CO, H_2O, and H_2S GGA Adsorption Energies (kcal/mol) As Obtained from Saturated (PS) and PC-Embedded (PC) Clusters, Compared with Experimental Values Obtained from Nearly Perfect TiO_2(110) Surfaces

	CO	H_2O	H_2S
PC (+4/−2)	26.5	67.3	
PC (+2/−1)	20.6	55.5	
PC (+2/−1) (BSSE)	17.9	53.2	
PS	8.8	20.8	8.7
PS (BSSE)	6.7	19.3	7.0
exptl	9.9[a]	17.0[b]	

[a] From ref 34. [b] From ref 37.

Not only does the theoretical trend closely follow the experimental one, but also the quantitative agreement is very good for all of the cases examined so far. Because the ionicities and structures of these materials are rather different, we infer that local effects play a dominant role in oxide−CO surface interactions.

To study the adsorption energetics, we performed GGA calculations using the LDA-optimized geometry, because LDA is known to considerably overestimate chemisorption energies.[23] The GGA adsorption energy is found to be 8.8 kcal/mol (∼11 kcal/mol lower than the LDA value). Inclusion of BSSE corrections lowers this value to 6.7 kcal/mol. This is slightly lower than the 9.9 kcal/mol found in the most recent experiment of Linsebigler, Lu, and Yates,[34] possibly because of the underestimation of the Madelung field because of the small dimensions of our model.[35] To check this hypothesis, we repeated our calculations embedding the model cluster in the PC fields already used in the previous calculations on the bare surface. The geometries were taken from the calculations with the saturators. Similarly to the calculations of Pacchioni et al.[5] the adsorption energy is now found to be much higher, i.e., 26.5 and 20.6 kcal/mol (without BSSE corrections) for the (4/−2) and for (2/−1) cases, respectively, and when correcting for the BSSE, the adsorption energy is too high (17.9 kcal/mol), even in the more favorable (+2/−1) case. It appears, therefore, that the negative effects due to the introduction of the Madelung field through the PC array are much heavier than those introduced by neglecting the field in the model adopting the pseudo-hydrogen saturators. This agrees with very recent calculations carried out on MgO by Pelmenschikov et al.[36] It is also remarkable that the (+4/−2) array seems to perform better than the (+2/−1) one when the DOS of the clean surface are considered wereas the opposite is true when looking at the adsorption energetics. This reflects the double role played by the embedding PCs, which, the one hand, act on the cluster DB states and, on the other, directly influence the adsorbate with their electrostatic field. All of the adsorption energies discussed in this section and those pertinent to H_2O and H_2S are collected in Table 4. In the same table, we also report data referring to recent experiments carried out on well-prepared TiO_2(110) surfaces.[34,37,38]

Through the use of Ziegler's transition-state method (see Table 5), we can analyze the nature of the interaction between the surface and the adsorbate. This method shows that the most important contribution to this interaction comes from the electrostatic term. However, this is largely offset by the Pauli repulsion, so that orbital bonding contributions are decisive. Among these orbital interaction terms, the σ (a_1) contribution is dominant, and the π contributes (b_1 and b_2 in Table 5), though sizable, are much weaker. This indicates that the importance of the π back-donation mechanism is minor; and this is confirmed by Table 6, where the Mulliken gross populations of CO are

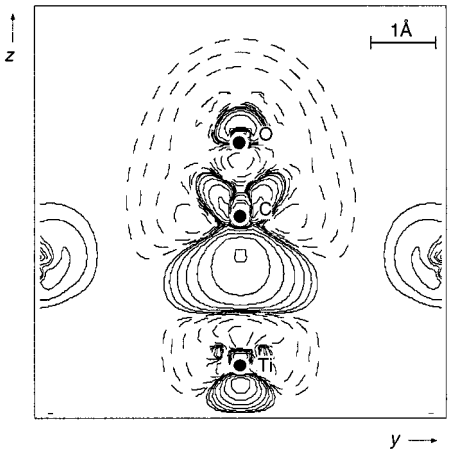

Figure 4. Plot (*yz* section) of the difference between the SCF electron density and the sum of the electron charge of the constituent fragments for the CO-adsorbed model cluster. Contour levels are $\pm 2 \times 10^{-4}$, $\pm 4 \times 10^{-4}$, $\pm 8 \times 10^{-4}$, ..., $\pm 1.28 \times 10^{-2}$ e/b^3. Negative levels are represented by dashed lines.

TABLE 5: Theoretical CO, H_2O, and H_2S GGA Adsorption Energies (kcal/mol) Decomposed following Ziegler's Transition-State Analysis

	CO	H_2O	H_2S
ΔE_{Pauli}	45.53	23.12	11.28
ΔE_{elstat}	−31.74	−31.02	−9.99
ΔE_{a_1}	−16.46	−10.87	−6.86
ΔE_{a_2}	−0.08	−0.18	−0.05
ΔE_{b_1}	−0.38	−2.17	−1.66
ΔE_{b_2}	−3.17	−1.58	−1.00
$\Delta E_{\text{prep,mol}}$	0.57	0.18	0.30
$\Delta E_{\text{prep,surf}}$	1.50	1.36	1.44

TABLE 6: Gross Mulliken Populations Before/After CO Adsorption as Found from Calculations on Clusters Terminated by Pseudo-hydrogen Saturators

orbital	C	O
s	1.76/1.52	1.84/1.88
p_σ	0.89/0.91	1.48/1.43
p_π	0.99/1.06	2.90/2.95
d	0.08/0.08	0.06/0.06
total	3.72/3.57	6.28/6.23

reported before/after the interaction with the surface: both the s and the p_σ C populations decrease because of the σ donation, but the p_π C population increases slightly. The overall charge resulting on the CO fragment is +0.20. The CO → surface donation process can also be appreciated in Figure 4, where a map of the difference between the charge of the interacting system and that of the noninteracting fragments is reported. The complexity of the charge rearrangement is a further indication of the importance of the covalent interaction.

The preceding analysis is confirmed by the DOS and COOP diagrams reported in Figures 5 and 6, where, according to the CO → surface charge donation, the 5σ MO is found to be strongly stabilized whereas the 1π MO is less affected. Incidentally, it is interesting to note in Figure 5b the presence of another component with a large 5σ character at ∼−10 eV, which should not be expected on the basis of a simple CO → Lewis acid site charge-donation scheme. This peak has a CO−surface antibonding character (see Figure 6a), which is not due to an interaction with Ti (see Figure 6b) but to a repulsion between the CO 5σ MO and the dangling bonds of the neighboring O_{II} oxygens (see Figure 6c). This could explain, at least partially, the weakness of the CO bonding to the surface.

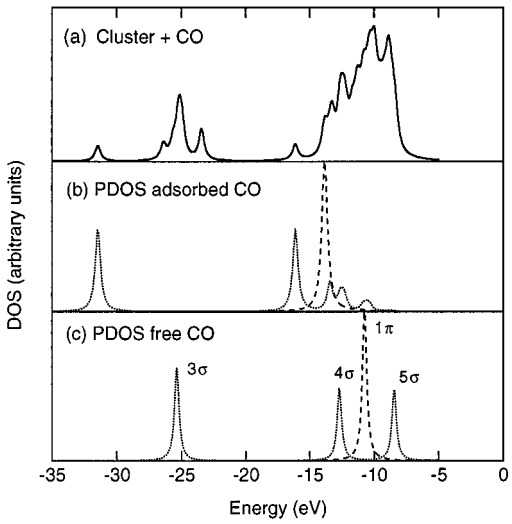

Figure 5. (a) DOS of the CO-adsorbed model cluster. (b) σ and π PDOS of the free CO molecule. (c) σ and π PDOS of the CO-adsorbed model cluster. Only occupied states are displayed in this panel.

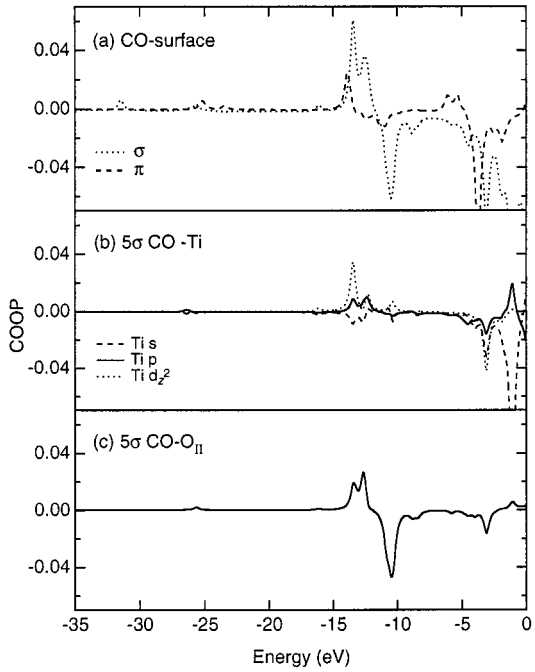

Figure 6. (a) COOP between CO and the surface. (b) COOP between the 5σ CO MO and the central Ti atom. (c) COOP between the 5σ CO MO and the bridging O_{II} atoms. Bonding (antibonding) states are represented by positive (negative) peaks.

When we compare our results with other recent first-principles calculations, we find that our estimate of molecular CO adsorption energy is rather close to those inferred from supercell calculations based on slab (5−12,[14] 11.1 kcal/mol[5]) and on polymer (9.1 kcal/mol[39]) models. For the cluster calculations, our predictions agree quite well with calculations adopting saturation with fitted multipoles by Reinhardt et al. (5−11 kcal/mol[14]), and they are considerably lower than calculations based on point-charge array termination (14−22,[14] 18−32[5] kcal/mol). Finally, our estimate for the C−O stretching frequency shift compares much better with experimental data than those reported in ref 39 (112 cm^{-1}) and in ref 5 (130−150 cm^{-1}). Although this could be explained in the latter case by the presence of the point charges, in the former it is probably due to the inadequacy of the Hartree−Fock approximation adopted therein.[24]

TABLE 7: Structural and Vibrational Properties of Free and Adsorbed (Saturated Cluster) H_2O As Obtained from LDA Calculations

	theor	exptl
free H_2O		
r_{OH} (Å)	0.972	0.957[a]
θ_{H_2O} (deg)	104.4	104.5[a]
υ_{asymOH} (cm^{-1})	3823	3756[a]
υ_{symOH} (cm^{-1})	3724	3657[a]
δ_{HOH} (cm^{-1})	1562	1596[a]
adsorbed H_2O		
r_{Ti-OH_2} (Å)	2.406	
Δz_{Ti} (Å)	−0.143	
r_{OH} (Å)	0.983	
θ_{H_2O} (deg)	107.5	
υ_{asymOH} (cm^{-1})	3674	
υ_{symOH} (cm^{-1})	3580	∼3420[b]
δ_{HOH} (cm^{-1})	1529	1605[b]
υ_{Ti-OH_2} (cm^{-1})	370	

[a] From ref 41. [b] From ref 42.

TABLE 8: Structural and Vibrational Properties of Free and Adsorbed (Saturated Cluster) H_2S As Obtained from LDA Calculations

	theor	exptl
free H_2S		
r_{OH} (Å)	1.367	1.336[a]
θ_{H_2S} (deg)	91.2	92.1[a]
υ_{asymSH} (cm^{-1})	2604	2684[b]
υ_{symSH} (cm^{-1})	2585	2611[b]
δ_{HSH} (cm^{-1})	1136	1290[b]
adsorbed H_2S		
r_{Ti-SH_2} (Å)	3.100	
Δz_{Ti} (Å)	−0.186	
r_{SH} (Å)	1.369	
θ_{H_2O} (deg)	94.7	
υ_{asymSH} (cm^{-1})	2593	
υ_{symSH} (cm^{-1})	2568	
δ_{HSH} (cm^{-1})	1110	
υ_{Ti-SH_2} (cm^{-1})	369	

[a] From ref 43. [b] From ref 44.

5. Molecular Adsorption of H_2O and H_2S

Both H_2O and H_2S were placed on the Ti Lewis acid site with their nucleophilic (O and S, respectively) end down. The adsorbate atoms were constrained in the (001) plane, viz., the *yz* plane of Figure 1, because explorative calculations showed that this is the preferred orientation. We point out that our calculations are *not* intended either to determine the actual geometry for molecular adsorption or to assess which form of adsorption (molecular or dissociative) is predominant: our model is probably too small for these purposes. It has actually been found from very recent DFT slab calculations[40] that in both issues interadsorbate interactions play a very important role. On the other hand, the configuration herein assumed for molecular adsorption has also been investigated for H_2O with DFT slab calculations,[10,40] which can be exploited to evaluate the reliability of our model. Structural and vibrational properties are reported in Tables 7 and 8 for H_2O and H_2S, respectively, together with available experimental reference data.[41−44]

For H_2O, the adsorption energy (19.3 kcal/mol, with BSSE corrections) is in excellent agreement with both the experiment value (17.0 kcal/mol) and that computed by Lindan et al.[40] with periodic slab calculations for the same configuration at θ = 0.5 (20.1 kcal/mol). This once more indicates a minor role for the interaction of the adsorbate with the surface Madelung field. By contrast, clusters embedded in the PC arrays yield dramatic overestimates of the adsorption energy, 53.2 kcal/mol in the

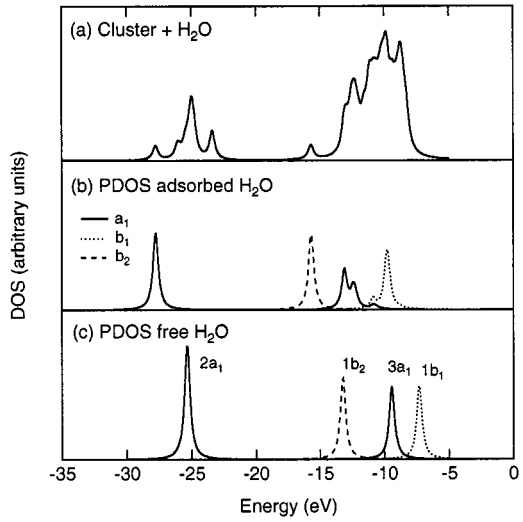

Figure 7. (a) DOS of the H_2O-adsorbed model cluster. (b) PDOS of the H_2O-adsorbed model cluster. (c) PDOS of the free H_2O molecule. Only occupied states are displayed in this panel.

most favorable (+2/−1) case. This is also found in investigations reported by other authors.[45]

For H_2S, the interaction with the surface is computed to be weaker ($\Delta H_{ads} = -7.0$ kcal/mol) than that of H_2O. This trend is in agreement with that found in recent periodic slab calculations for the TiO_2 anatase (101) surface,[46] where adsorption similarly occurs on 5-fold-coordinated Ti ions. The low adsorption energy for molecularly adsorbed H_2S indicates that dissociative adsorption should be highly favored for this species. It has been found by Beck et al.[47] that surface hydroxyl groups are readily formed when exposing powdered rutile TiO_2 samples to H_2S. We cannot report in this case adsorption energies for the PC-array-terminated clusters, because these calculations could not be acceptably converged. Problems were related to the high energy of H_2S lone pairs (see below) and to the well-known DFT band-gap underestimation.[48] This, along with the low efficiency of PCs in cleaning the gap energy region from spurious surface states, caused strong oscillations in the occupations of the cluster MOs.

As is true for CO, the molecule−surface interaction is largely dominated by the σ-donor interaction (see Table 5). From Mulliken population analysis, H_2O and H_2S are found to be positively charged (+0.15 and +0.20, respectively).

The DOS curves for H_2O are reported in Figure 7. The H_2O σ lone pair (i.e., the $3a_1$ MO) is stabilized with respect to the other valence levels. This agrees with the σ-donation mechanism inferred from the preceding analysis and with the difference synchrotron ultraviolet-photolelectron (UP) spectra obtained at 160 K by Kurtz et al.[49] The H_2O σ lone pair is also split into two components, as for CO, for analogous reasons. However, similar behavior is observed also for the π lone pair (the $1b_1$ MO) as well, which exhibits a small "satellite" at more negative binding energies. We can understand the origin of this feature by looking at Figure 8c, where the COOP between the $1b_1$ H_2O MO and the O_{II} p_z AOs are reported. The repulsion between the H_2O π lone pair and the dangling bond combinations of the 3-fold-coordinated surface oxygens is revealed by the large, negative peak at ∼−10 eV. A map of the main state contributing to this antibonding peak, confirming the repulsive nature of the interaction, is reported in Figure 9. Unfortunately, no reliable difference UP spectra in the region of the H_2O $1b_1$ state have been obtained[49] to be compared with our predictions. It is noteworthy, however, that the PDOS curves of Figure 7b

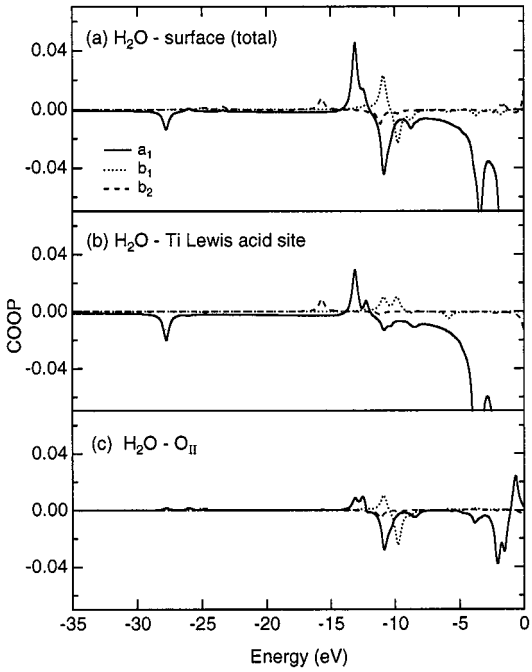

Figure 8. COOP between adsorbed H_2O and the surface and its contribution due to the interaction between the $1b_1$ H_2O MO and the O_{II} p_z AOs.

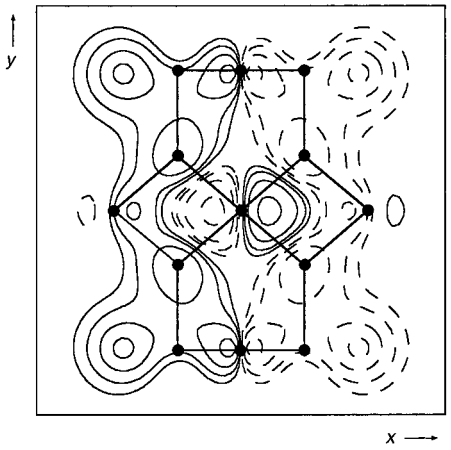

Figure 9. Plot (*xy* section, 2 b above the surface) of the state corresponding to the lowest energy peak of the adsorbed H_2O PDOS (Figure 10b). Contour levels are $\pm 2 \times 10^{-2}$, $\pm 4 \times 10^{-3}$, and $\pm 8 \times 10^{-3}$ $e^{1/2}/b^{3/2}$ .... Negative levels are represented by dashed lines. The skeleton of the cluster is projected for clarity (only Ti and O atoms are displayed).

perfectly match those obtained from DFT slab calculations by Goniakowski and Gillan[10] for molecularly adsorbed H_2O.

For H_2S, the DOS curves reported in Figure 10 show that the $2b_1$ sulfur lone pair is the HOMO of the surface complex, thus explaining the above-mentioned difficulty in converging the calculations for the PC-terminated cluster. Furthermore, the b_1 peak is not split in this case, this is related to the longer Ti−adsorbate distance for H_2S, which makes negligible the repulsive interaction with the lone pairs of the 3-fold oxygens.

An examination of the structure of the surface complexes shows that slight variations are found with respect to the noninteracting fragments. In particular, the Ti acid site undergoes a counter-relaxation, which is stronger for H_2O ($z = -0.143$ Å) than for H_2S ($z = -0.186$ Å). For the adsorbates, the bond angle opening is due to the increased contribution of the $1b_2$ (for H_2O) and $2b_2$ (for H_2S) MOs to the O−H (S−H) bonds,

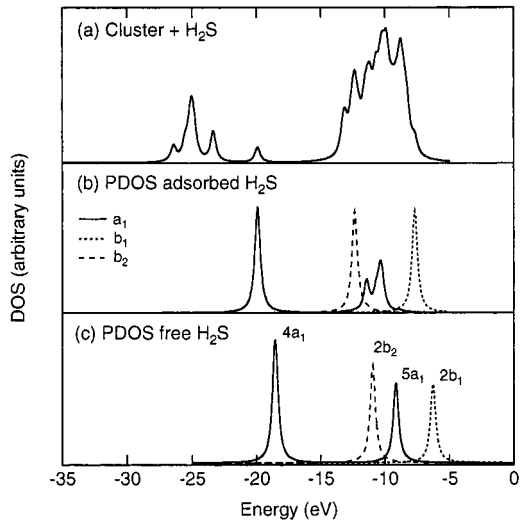

Figure 10. (a) DOS of the H_2S-adsorbed model cluster. (b) PDOS of the H_2S-adsorbed model cluster. (c) PDOS of the free H_2S molecule. Only occupied states are displayed in this panel.

which is, in turn, related to the involvement of the $3a_1$ ($5a_1$) MOs in the surface−adsorbate bonding.

For the vibrations of the adsorbates, a comparison with the experiment is possible only for H_2O.[42] We correctly find a strong redshift of the OH stretching frequency, consistent with the σ-electron charge withdrawal from the molecule. However, although we predict that the HOH scissoring mode should also undergo a redshift, a small blueshift is found experimentally. A possible explanation for this discrepancy is that molecular adsorption of H_2O does not occur in the simple way we assume in our calculations but that additional weak interactions (either with other adsorbed species or with surface sites) are present. The possibility that molecularly adsorbed H_2O could be involved in weak interactions with other adsorbates was already suggested by Lindan et al.[50] to explain the contradictions between slab calculations[10] and most recent experimental studies. High-resolution electron energy loss spectroscopy,[51] temperature-programmed desorption with isotope labeling,[52] and modulated molecular beam scattering[53] experiments carried out on the (110) surface of TiO_2 monocrystals clearly indicate that molecular adsorption of H_2O is predominant. Important theoretical evidence supporting this picture has been obtained in very recent DFT slab calculations, which H_2O molecular adsorption is found to be significantly stabilized by the formation of hydrogen bonds with surface OH groups.[40]

6. Conclusion

Our density functional calculations show that a small Ti_7O_9 cluster saturated with pseudo-hydrogens is able to model realistically the behavior of the Ti^{4+} Lewis acid site of the TiO_2 rutile (110) surface. Chemisorption energies compare well with experimental values for all of the examined probe molecules (CO, H_2O, and H_2S). The bonding interaction is found to be dominated by the σ-charge donation from the adsorbate, and long-range effects because of the Madelung potential seem to be of minor importance. The existence of significant repulsions between adsorbates and surface dangling bonds has been shown. As in the analogous studies we previously carried out on other oxide surfaces, the computed CO stretching-frequency shift is in excellent agreement with that of the experiment. For H_2O, the frequency of the HOH scissoring mode is found to be incorrectly redshifted. This discrepancy can be explained by admitting that, besides interacting with the Ti^{4+} Lewis acid site, molecularly adsorbed water is also involved in weak interactions with other adsorbed species, as found in very recent slab calculations.

Acknowledgment. This work is supported by the "Progetto Finalizzato Materiali Speciali per Tecnologie Avanzate II", funded by CNR (Rome).

References and Notes

(1) Fujishima, A.; Honda, K. *Nature* **1972**, *238*, 37.
(2) Linsebigler, A. L.; Lu, G.; Yates, J. T., Jr. *Chem. Rev.* **1995**, *95*, 735.
(3) Charlton, G.; Howes, P. B.; Nicklin, C. L.; Steadman, P.; Taylor, J. S. G.; Muryn, C. A.; Harte, S. P.; Mercer, J.; McGrath, R.; Norman, D.; Turner, T. S.; Thornton, G. *Phys. Rev. Lett.* **1997**, *78*, 495.
(4) Ramamoorthy, M.; Vanderbilt, D.; King-Smith, R. D. *Phys. Rev. B* **1994**, *49*, 16721.
(5) Pacchioni, G.; Ferrari, A. M.; Bagus, P. S. *Surf. Sci.* **1996**, *350*, 159.
(6) Casarin, M.; Tondello, E.; Vittadini, A. *Surf. Sci.* **1994**, *303*, 125.
(7) Casarin, M.; Maccato, C.; Vittadini, A. *Surf. Sci. Lett.* **1997**, *387*, L1079.
(8) Casarin, M.; Favero, G.; Tondello, E.; Vittadini, A. *Surf. Sci.* **1994**, *317*, 422.
(9) Casarin, M.; Maccato, C.; Vittadini, A. *Chem. Phys. Lett.* **1997**, *280*, 53.
(10) Goniakowski, J.; Gillan, M. J. *Surf. Sci.* **1996**, *350*, 145.
(11) Burdett, J. K.; Hughbanks, T.; Miller, G. J.; Richardson, J. W., Jr.; Smith, J. V. *J. Am. Chem. Soc.* **1987**, *109*, 3639.
(12) Bredow, T.; Jug, K. *Surf. Sci.* **1995**, *327*, 398.
(13) Hirshfeld, F. L. *Theor. Chim. Acta* **1977**, *44*, 129. Wiberg, K. B.; Rablen, B. R. *J. Comput. Chem.* **1993**, *14*, 1504.
(14) Reinhardt, P.; Causà, M.; Marian, C. M.; Hess, B. A. *Phys. Rev. B* **1996**, *54*, 14813.
(15) Casarin, M.; Maccato, C.; Vittadini, A. *Appl. Surf. Sci.*, in press.
(16) Bredow, T.; Geudtner, G.; Jug, K. *J. Chem. Phys.* **1996**, *105*, 6395.
(17) Vittadini, A.; Selloni, A. *Phys. Rev. Lett.* **1995**, *75*, 4756.
(18) We adopt for the PC field here the same notation as that used in ref 5.
(19) *Amsterdam Density Functional Package*, Version 2.0.1; Vrije Universiteit: Amsterdam, The Netherlands, 1996; Version 2.3.0, Vrije Universiteit: Amsterdam, The Netherlands, 1997.
(20) Baerends, E. J.; Ellis, D. E.; Ros, P. *Chem. Phys.* **1973**, *2*, 41. te Velde, G.; Baerends, E. J. *J. Comput. Phys.* **1992**, *99*, 84. Fonseca Guerra, C.; Visser, O.; Snijders, J. G.; Baerends, E. J. In *Methods and Techniques in Computational Chemistry*; Clementi, E., Corongiu, G., Eds.; STEF: Cagliari, Italy, 1995; Chapter 8, p 305.
(21) Becke, A. D. *Phys. Rev. A* **1988**, *38*, 3098. Perdew, J. P. *Phys. Rev. B* **1986**, *33*, 8822.
(22) Ziegler, T. *Chem. Rev.* **1991**, *91*, 651.
(23) White, J. A.; Bird, D. M.; Payne, M. C.; Stich, I. *Phys. Rev. Lett.* **1994**, *73*, 1404. Gundersen, K.; Jacobsen, K. W.; Nørskov, J. K.; Hammer, B. *Surf. Sci.* **1994**, *304*, 131. Philipsen, P. H. T.; te Velde, G.; Baerends, E. J. *Chem. Phys. Lett.* **1994**, *226*, 583. Hu, P.; King, D. A.; Crampin, S.; Lee, M. H.; Payne, M. C. *Chem. Phys. Lett.* **1994**, *230*, 501.
(24) Ziegler, T.; Rauk, A. *Theor. Chim. Acta* **1977**, *46*, 1.
(25) Rosa, A.; Ehlers, A. W.; Baerends, E. J.; Snijders, J. G.; te Velde, G. *J. Phys. Chem.* **1996**, *100*, 5690.
(26) Hoffmann, R. *Solids and Surfaces: A Chemist's View of Bonding in Extended Structures*; VCH: New York, 1988.
(27) Vogtenhuber, D.; Podloucky, R.; Neckel, A.; Steinemann, S. G.; Freeman, A. J. *Phys. Rev. B* **1994**, *49*, 2099.
(28) Reinhardt, P.; Hess, B. A. *Phys. Rev. B* **1994**, *50*, 12015.
(29) Bates, S. P.; Kresse, G.; Gillan, M. J. *Surf. Sci.* **1997**, *385*, 386.
(30) It is well-known that on low-index faces of oxides CO is always adsorbed through the carbon end down on surface cations. See: Zecchina, A.; Scarano, D.; Bordiga, S.; Ricchiardi, G.; Geobaldo, F. *Catal. Today* **1996**, *27*, 403.
(31) Huber, K. P.; Herzberg, G. *Constants of Diatomic Molecules*; Van Nostrand Reinhold: New York, 1979.
(32) Hadjiivanov, K.; Davidov, A.; Klissurski, D. *Kinet. Katal.* **1988**, *29*, 161. Busca, G.; Saussey, A.; Saur, D.; Lavalley, J. C.; Lorenzelli, V. *Appl. Catal.* **1985**, *14*, 245. Morterra, C.; Garrone, E.; Bolis, V.; Fubini, B. *Spectrochim. Acta, Part A* **1987**, *43*, 1577.
(33) Vahrenkamp, H. *Struct. Bonding (Berlin)* **1977**, *32*, 11. Zecchina, A. Personal communication. Scarano, D.; Galletto, P.; Lamberti, C.; De Franceschi, R.; Zecchina, A. *Surf. Sci.* **1997**, *387*, 236.

(34) Linsebigler, A.; Lu, G.; Yates, J. T., Jr. *J. Chem. Phys.* **1995**, *103*, 9438.

(35) A ∼5% increase of the adsorption energy is found when taking a substantially larger $Ti_{19}O_{32}$ cluster.[15]

(36) Pelmenschikov, A. G.; Morosi, G.; Gamba, A.; Coluccia, S. *J. Phys. Chem. B* **1998**, *102*, 2226.

(37) Hugenschmidt, M. B.; Gamble, L.; Campbell, C. T. *Surf. Sci.* **1994**, *302*, 329.

(38) We take into consideration here only recent experiments carried out on nearly perfect (110) surfaces. Previous determinations of adsorption energies, made either on powdered samples or on oxidized metal foils, give significantly higher values and are probably affected by the presence of defects.

(39) Fahmi, A.; Minot, C. *J. Organomet. Chem.* **1994**, *478*, 67.

(40) Lindan, P. J. D.; Harrison, N. M.; Gillan, M. J. *Phys. Rev. Lett.* **1998**, *80*, 762.

(41) Eisemberg, D.; Kauzmann, W. *The Structure and Properties of Water*; Oxford University Press: New York, 1969.

(42) For example, see: Griffiths, D. M.; Rochester, C. H. *J. Chem. Soc., Faraday Trans. 1* **1977**, *73*, 1510.

(43) Huheey, J. E. *Inorganic Chemistry: Principles of Structure and Reactivity*, 2nd ed.; Harper and Row: New York, 1978.

(44) Herzberg, G. *Molecular Spectra and Molecular Structure*; Van Nostrand: New York, 1949; Vol. 2.

(45) Ahdjoudj, J.; Minot, C. *Surf. Sci.* **1998**, *402*−*404*, 104.

(46) Selloni, A.; Vittadini, A.; Grätzel, M. *Surf. Sci.* **1998**, *402*−*404*, 219.

(47) Beck, D. D.; White, J. M.; Ratcliffe, C. T. *J. Phys. Chem.* **1986**, *90*, 3123.

(48) Parr, R. G.; Yang, W. *Density-functional theory of Atoms and Molecules*; Oxford University Press: New York, 1989.

(49) Kurtz, R. L.; Stockbauer, R.; Madey, T. E.; Román, E.; De Segovia, J. L. *Surf. Sci.* **1989**, *218*, 178.

(50) Lindan, P. J. D.; Harrison, N. M.; Holender, J. M.; Gillan, M. J. *Chem. Phys. Lett.* **1996**, *261*, 246.

(51) Henderson, M. A. *Surf. Sci.* **1996**, *355*, 151.

(52) Henderson, M. A. *Langmuir* **1996**, *12*, 5093.

(53) Brinkley, D.; Dietrich, M.; Engel, T.; Farrall, P.; Gantner, G.; Schafer, A.; Szuchmacher, A. *Surf. Sci.* **1998**, *395*, 292.